IRAQI
Academic Scientific Journals

Optimization of nanoparticles concentration by using turbidity in solar still

Khaoula hidourI[1],   Ali Benhmidene[1],   Hanen Ajari [1]

[1]Laboratory of energy, water and environment (LEEEP), Engineers National School of Gabes, Gabes University, Omar Ibn El Khattab Street, 6029 Gabès, Tunisia

ABSTRACT

The present work we know referred to an experimental approach based on an optimization of the range of nanoparticle fraction in the solution guaranteeing a homogeneous solution by measuring the turbidity each time. Thus, a better intervention of nanofluid without coagulations in the work basin of our distiller. One of the parameters influencing the efficiency of nanoparticles is optimizing working concentrations. An increase in turbidity decreases water production. The turbidity measured either in the order 238FNU was noticed constant after a time of 2h30 continued measurement after a suitable rest time of 30 minutes if our solution keeps the same turbidity of the solution corresponding to a concentration less than or equal to 0.01%. The nanoparticles of Al_2O_3 and Cu_2O give better production values for low concentrations ranging from 350-500mL/h for Al_2O_3 and in the range 300-700mL / h that of Cu_2O

Introduction

Desalination technologies have become increasingly used to improve the quality and quantity of water day after day. At our days the use of clean energy especially solar energy for water desalination has received a lot of attention. However, de quantity that is produce in use solar still insufficiency. One of the techniques recently studied to improve productivity consists in dispersing nanoparticles in brackish. This context, Kabeel el al. (2014) studied the effect of adding Al_2O_3 nanoparticles to water in a simple solar still with external condenser at 0.2% and they improve that the productivity was increased by 116% [1]. Elango el al. (2015) improves in their study that Al_2O_3 nanofluids enhanced productivity by 29.9%. Sahota and Tiwari (2016a) are used three types of nanoparticles namely Al_2O_3, TiO_2 and CuO under the climatic conditions of New Delhi in India with 0.25%. They have the thermal energy efficiencies for the still were 50.34%, 46.10%, and 43.81% for Al_2O_3, TiO_2, and CuO respectively, while the thermal energy efficiencies for the water-only solar still were 37.78%. Thus, Al_2O_3 was found to be the most efficient nanoparticles, achieving the greatest increase in thermal energy efficiency. The productivity of the solar still with Al_2O_3 was higher followed by TiO_2 and CuO, for all weather conditions. Panitapu et al. (2014) realized in experimental study on simple solar still using titanium oxide (TiO_2) nanoparticles in Hyderabad, India. The results show that the temperatures of the water, the basin, the transparent cover inside than outside are higher with the use of titanium nanoparticles compared of water only. They therefore stated that titanium oxide is a promising nanoparticle that contributes to the improvement of the productivity of the distiller. Kabeel, Omara and Essa (2014a, 2014b) experimentally studied the performance two types of solar still with cuprous oxide (Cu_2O) and aluminum oxide (Al_2O_3) at Kafrelsheikh University in Egypt. The results claim that the use of the external condenser increases the productivity of the distiller only by 53.2%, while the productivity of the still is increased by 133.64% and 125.0% with vacuum for Cu_2O and Al_2O_3 respectively, and 93.87% and 88.97% without vacuum compared to the conventional still. Thus the Cu_2O nanoparticle is considered an effective nanoparticle. The Results found by the researchers show that the nanoparticles of alumina Al_2O_3, copper oxide CuO, dicopper oxide Cu_2O and titanium dioxide are proven to be the best nanoparticles that can increase the productivity of a solar still. Therefore, we will choose as study nanoparticles, alumina Al_2O_3 and dicopper oxide Cu_2O. The study of Kalpeshkumar et al (2020)The addition of AL2O3 with a concentration of the order of 0.1% for different depths of water 30mm,

20mm and 10mm gave an equal production of 19.4%, 28.53% and 26.59% respectively. Using CuO for depths of 20mm and 10mm they found 58.25% and 56.38% respectively. Two identical solar distillers were made by Mohamed et al (2021) in order to add different concentrations of two types of nanoparticle with the same working conditions and at the same time. The CuO with a concentration of 0.6% gave an efficiency of 9.62% while that of AL2O3 with a concentration of 0.4% gave an efficiency which does not exceed 7.8%.. The output of the still with graphite and CuO nanofluid reached approximately 41.18% and 32.35 %, respectively, over the classical one this resulats it be given by Kalpeshkumar et a (2020) . The diurnal energy efficiency of graphite and CuO nanofluids is 41.18% and 38.61%, respectively, and for CSS is 29.17%. Two identical solar stills were made by Mohamed A et al (2021) in order to add different concentrations of two types of nanoparticle with the same working conditions and at the same time. The CuO with a concentration of 0.6% gave an efficiency of 9.62% while that of Al2O3 with a concentration of 0.4% gave an efficiency which does not exceed 7.8%. Several research works have used different types of nanoparticles, thereafter a comparative study has each time been made to know the difference in the production of distilled water between a conventional solar still and one hybridized with nanoparticles. The following histogram (Fig.1) gives some results for this work. All researchers have proven that the addition of nanoparticles aims to increase the productivity, whatever the nature of the nanoparticles (Kou et al (2019) Kabeel et al (2019). Satori et al (2014) Du et al (2018) Afes et al (2018)). Mojarrad et al. (2014) prepared Al2O3-water nanofluids using the two-way method steps. Khairul et al. (2016) also prepared Al2O3-water nanofluids by the method in two step. Das et al. (2017) carried out an experimental study on the use of surfactants in the preparation of the Al2O3-water nanofluid, proceeding the two-step method. Soltani and para. (2010) first prepared the base liquid, then the nanoparticles were added and thoroughly mixed for 6 h. Duangthongsuk and Wongwises prepared TiO2 and Al2O3 nanofluids by dispersing the nanoparticles in distilled water, with a ultrasonic shaking for 20 min and continuous ultrasonication for 30 min. Sajadi and Kazemi have mixed the right amount of TiO2 nanoparticles with distilled water by a mixer for 10 min. Next, an ultrasonic cleaner was used to disperse the nanoparticles for 30 min. kabeel et al. (2014) experimentally studied improving the performance of the solar still by using Cu2O and Al2O3 nanofluids, prepared by the two-step method, and providing vacuum. Subsequently, the two-step method will be chosen as the method for preparing the nanofluids to be studied. To proceed with the preparation of the

nanofluids, we first started with a preliminary study to ensure the stability of these nanofluids, which is the measurement
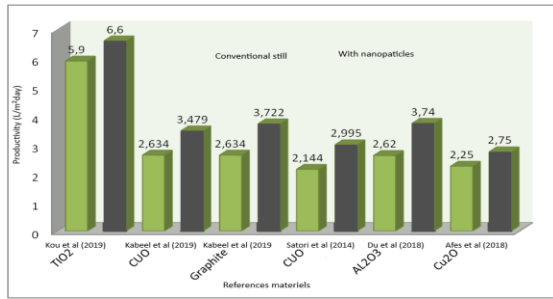

Fig. (1): Histogram of productivity in function with references

of the turbidity of the nanoparticle/seawater mixture. The nanoparticles were all spherical in shape and the purity was at least 99.5%. It is crucial to determine the diameters of these nanoparticles, for this we passed each nanoparticle through a set of sieves with diameters ranging from 250 mm to 40 micrometers. The two nanoparticles of Al2O3 and Cu2O have a diameter between 63 and 50 micrometers.

1. Photovoltaic Theory

This part aims to give the configuration of solar distillation using a simple solar still coupled to a heat pump in the presence of nanoparticles added to seawater. This configuration makes it possible to determine the temperatures of the various components of the still as well as the hourly production of distilled water. As shown in Fig.2 and 3, this is a still comprising essentially a basin whose bottom and walls are insulated, a glass cover inclined 30% horizontally to condense the water vapor produced. The distilled water produced is collected using a collecting channel at the bottom of the basin. A heat pump is used to improve the temperature of the water in the basin (having the same dimensions of that used in a single still) to increase evaporation and improve condensation of the distillate. This model corresponds to a cold compression cycle. A condenser is immersed in the basin to increase the temperature of the water, so the amount of evaporated water will increase. The evaporator which is located near the upper part of the glass cover improves the condensation of water vapor and refrigerant after leaving the condenser. After that, the refrigerant enters the evaporator at the low pressure inducing the condensation of water vapor. As a result, more condensed water will be collected at the distilled water gutter. The thermal and mass balances, shown down, are studied both experimental and then solved numerically in MATLAB by using ODEO23 method under climatic conditions of the region of

Gabes, south Tunisia, during a typical days of June 24,25 and 26 June 2021.
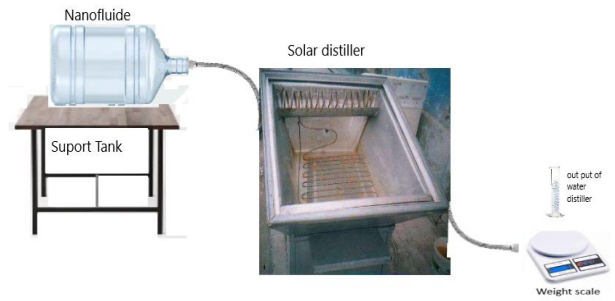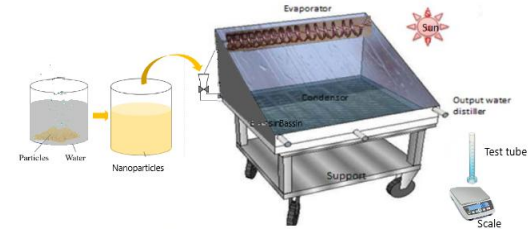

Fig. (2): Photo of experimental setup

Fig. (3): Schematic diagram of hybrid solar still

2. Nanoparticles preparations:

The nanoparticles in the base fluid are stirred using a magnetic stirrer also called an ultrasonic bath. A homogeneous mixture is obtained. The assembly clearly shows the sonication method by ultrasonic agitation at two stages of nanofluid preparation, Fig. 4. Ultrasonic waves are used for the purpose of increasing mixing stability. Typical ultrasound probe exceeds an ultrasonic bath by a factor of 1,000 through focusing and uniform ultrasonic power input
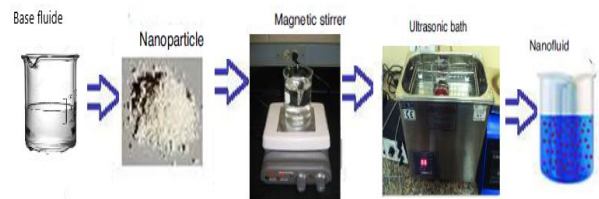

Fig. (4) Nanofluids preparations

3.Uncertainty analysis

The measurements of the parametric variables, air flow rate, water temperature, water level and relative air humidity and temperature within the basin inlet and on the water surface, were taken during the experiments. The water temperature in the basin was

measured using the thermometer-Pt100, which works in the range from −20 to +260ºC with an uncertainty of 2.6%. The relative humidity and temperature of air streams were measured using 2 thermo-hygrometers which work in the range from 0 to 100% RH and from−40 to+120ºC and its uncertainty is 1.4%. scale has a measurement uncertainty of 1mg, and you measure 10g, the result should be 10±0.01%.

5. Turbidity measurement:

The HI847492 Haze Meter is a portable, high-accuracy meter for analyzing impure water. The HI847492 is ASBC (American Society of Brewing Chemists) compliant. The meter is specifically designed for quality measurement and providing accurate, precise readings every time (Fig 5). The nanoparticles were all spherical in shape and the purity was at least 99.5% and they have a diameter between 50 and 63 nanometers. To ensure good dispersion and stability of the nanoparticles in the base fluid, the preparation of the nanofluids is carried out as follows: the Cu_2O nanoparticles are first measured using a balance. They are then injected and mixed with the base fluid (seawater) using a magnetic stirrer while measuring, for every 30 minutes, the turbidity of the mixture for different values of the concentration of the nanoparticles, to highlight the concentration with which the nanofluid remains stable during and after shaking. The results of the measurement of the turbidity of the nanofluid are grouped together in the following tables. Table1 gives the values of the turbidity of the nanoparticle/seawater mixture for each 30 minutes of agitation for φ=0.05%. After 2 hours and 30 minutes of slow magnetic agitation, we can see that the turbidity becomes almost constant. Stirring stops for 30 minutes and the turbidity is measured again. It decreases to the value of 206 FNU. So, with the concentration of 0.05%, the mixture is not stable.

Table 1: Turbidity of nanofluid after agitation for φ=0,05%

Time of agitation (h)	t_0 = 0	t1= 30min	t2= 1h	t3= 1h : 30 min	t4= 2h	t5= 2h : 30 min	t6= 3h	t7= 3h: 30 min
Turbidity (FNU)	2, 13	723	732	763	801	814	820	825

And therefore, the concentration of nanoparticles in the base fluid must be reduced until the stability of the mixture is reached. The following tables group together the different values of the turbidity of the nanofluid after a stirring time equal to 3 hours and 30 minutes (Table 2).

Table 2: Turbidity of nanofluid after agitation for φ=0,04%

Time of agitation (h)	t_0 =0	t1= 30 min	t2= 1h	t3= 1h : 30 min	t4= 2h	t5= 2h : 30 min	t6= 3h	t7= 3h: 30 min
Turbidity (FNU)	2, 13	524,3	558	583	613	633	645	656

For the three concentrations 0.04%; 0.03% and 0.02%, the turbidity becomes stabilize after a stirring time equal to 3 hours and 30 minutes. For each concentration, the turbidity value is measured again after a rest time always equal to 30 minutes (Table 2,3 and 4), For φ=0.04%; φ=0.03% and φ=0.02% the turbidities are 250 FNU, 299 FNU and 350 FNU respectively. There are also deposits at the bottom of the beaker. One must proceed, then, to a lower level of concentration.

Table 3: Turbidity du nanofluid after agitation for φ=0,03%

Time of agitation (h)	t_0 = 0	t1= 30min	t2= 1h	t3= 1h : 30 min	t4= 2h	t5= 2h : 30 min	t6= 3h	t7= 3h: 30 min
Turbidity(FNU)	2, 13	461,9	483,5	517	530	547	553	567

Table 4: Turbidity of nanofluid after agitation for φ=0,02%

Time of agitation (h)	t_0 = 0	t1= 30min	t2= 1h	t3= 1h : 30 min	t4= 2h	t5= 2h : 30 min	t6= 3h	t7= 3h: 30 min
Turbidity(FNU)	2, 13	319,5	329	361,5	387,7	419	426,2	430,5

Table 5 gives the values of the turbidity of the nanofluid during magnetic stirring for φ=0.01%, After 2 hours of slow stirring, it is observed that the turbidity of the mixture becomes stable, so the stirring is stopped and the turbidity is measured again. It is found that the value of the turbidity does not very much, it becomes 245 FNU after 30 minutes of rest. After 1 hour of rest, the turbidity is 238.

Table 5: Turbidity du nanofluid after agitation for φ=0,01%

Temps of agitation (h)	t_0 =0	t1= 30min	t2= 1h	t3= 1h : 30 min	t4= 2h	t5= 2h : 30 min	t6= 3h	t7= 3h: 30 min
Turbidity (FNU)	2,13	185	198,7	214	238	238	238	238

Therefore, and to guarantee the stability of the nanofluid, one must work with concentrations less than or equal to 0.01%. To confirm this result, the same procedure for preparing the nanofluid is repeated for φ=0.005%. Table 6 gives the turbidity values of the nanoparticle/seawater mixture with φ=0.005% for each 30 minutes of slow stirring. After 30 min of stopping the agitation, the turbidity is 133 FNU, after 1 hour, it is around 128. It is concluded, according to tables 1, 2, 3, 4, 5 and 6, that the seawater/nanoparticle mixture becomes stable for a concentration less than or equal to 0 .01%. Even after stopping the agitation, the nanoparticles remain in suspension and there is no settling. Consequently, the concentrations of the nanoparticles in the base fluid (sea water) will be chosen to be less than or equal to 0.01%. To guarantee the stability of nanofluids, the concentrations of nanoparticles in seawater have therefore been set at 0.01%; 0.0075% and 0.005% for each type of nanoparticle. The preparation of nanofluids requires the guarantee of good dispersion and stability of the nanoparticles in the base fluid during the experiment.

Table 6: Turbidity of the nanofluid during stirring for φ=0.005%.

Time of agitation (h)	t_0 = 0	t1= 30 min	t2 =1 h	t3 =1 h : 30 min	t4 =2 h	t5 =2 h : 30 min	t6 =3 h	t7 =3 h: 30 min
Turbidity(FNU)	2,13	54,5	72,9	89,8	109	138	138	138

5. Results

Three summer days were selected and presented as part of this study. The main meteorological parameters characterizing the test day, namely: solar irradiation, ambient temperature and wind speed, are illustrated in Fig.6. During the summer test days (24-25-26/06 /2022), the ambient temperature reaches 25°C. The

wind speed varies between 2 and 6 m/s. Figure 7 represents the variation of global solar radiation for 11 hours (from 8 a.m. to 6 p.m.) and for clear weather, it can be seen that at 8 a.m., the sunshine is generally low, its intensity increases with sunrise to reach its maximum at noon (exceeds 1000 W/m²) and it continues to decrease until sunset.
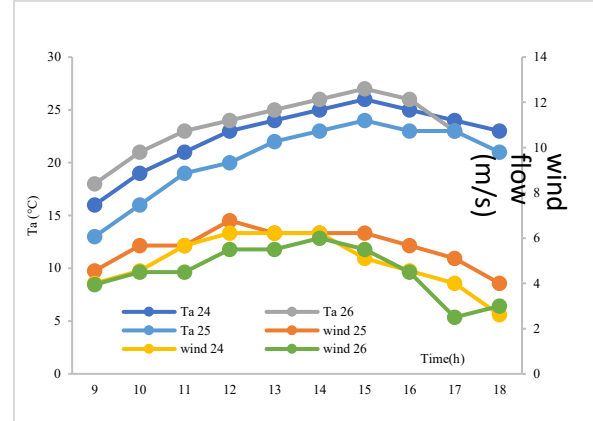

Fig. (5): Evolution of ambient temperature and wind velocity 24-25-26 June 2021
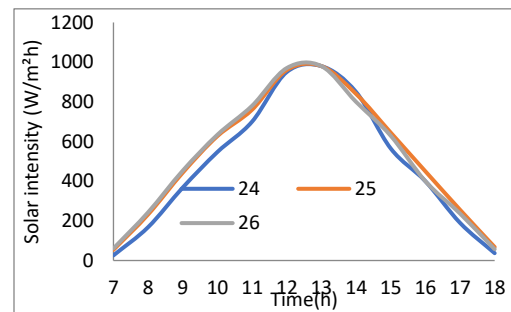

Fig. (6): Solar intensity 24-25-26 June 2021

6. Energy balances
6.1 Energy balance on the glass

The transparent cover receives solar radiation in the form of heat, absorbs a small part and transfers the major part to the nanofluid and basin assembly. The gradient temperature between the cover and the nanofluid, the latter transfers heat to it by evaporation, radiation and convection. In contact with the atmosphere, the transparent cover loses heat by convection and radiation. The thermal balance at the level of the cover is given by G. Peng et al (2018) by the following equation:

$$\frac{dT_g}{dt} = \frac{S_g}{(m_g C_{pg})}(\alpha_g G + (q_{e,nf-g} + q_{r,nf-g} + q_{c,nf-g}) - q_{r,g-sky} - q_{c,g-a})$$

6.2 Energy balance on the basin

The basin liner receives solar radiation transmitted through the transparent cover, absorbs some and

transfers some to the nanofluid as convective heat and releases some to the atmosphere as conductive heat. The heat balance over the basin below is given by Khaoula and Mohanraj (2019),

$$\frac{dT_b}{dt} = \frac{S_b}{(m_b C_{pb})}(\tau_g \tau_{nf} \alpha_b G - q_{c,b-nf} - q_{loss})$$

6.3 Energy balance on the nanofluid

As already mentioned, the nanofluid receives the solar radiation transmitted by the transparent cover, the convective heat of the basin and the heat transferred by the ashes (heat pump). Heat losses from the nanofluid include convective, radiative, and evaporative heat to the cover glass. The heat balance on the glass is as follows (G. Peng et al., 2018),

$$\frac{dT_{nf}}{dt} = \frac{S_{nf}}{(m_{nf} C_{pnf})}(\tau_g \alpha_{nf} G + q_{c,b-nf} - q_{r,nf-g} - q_{e,nf-g} - q_{c,nf-g} + q_{mnf})$$

6.4 Energy balance on the evaporator

The evaporator receives heat from the nanofluid by convection and evaporation and loses heat by convection, and since it is protected by a separating wall, the radiant heat transfer from the nanofluid to the evaporator is eliminated from the heat balance at the evaporator level (Hiba Akrout, 2021),

$$\frac{dT_e}{dt} = \frac{S_e}{m_e C_{pe}}(q_{c,nf-ev} + q_{e,nf-ev} - q_{pertes,ev})$$

6.5 Mass transfer

The quantity of water recovered is given by the following equation (Khaoula Hidouri, 2014)

$$\frac{dm_e}{dt} = \frac{q_{e,nf-g} + q_{e,nf-ev}}{h_{fg}}$$

6.6 Evaluation of heat exchange coefficients

6.7 Heat flux exchanged by convection

The rate of heat transfer by convection is given by the general equation (the fundamental law of convection)

Qc = h_c .ΔT.S

That is $\frac{Qc}{S} = hc.\Delta T$

And so q_c= h_c .ΔT

Where h_c is the convective transfer coefficient and S is the corresponding surface. We can then deduce that: The heat flux exchanged by convection between the glass and the ambient $q_{c,g-a}$ is given by:

$q_{c,g-a}$ = $h_{c,g-a}$ (T_g-T_a)

The heat lost from the pool to the atmosphere by conduction $q_{loss}$is given by Einstein (1956),

$q_{losses,b}$= Ki/Li(T_b-T_a)

Were

Ki and Li are the thermal conductivity and the thickness of the insulation and $h_{c,g-a}$ is the heat transfer coefficient by convection from the glass to the environment, given by the following relationships (Hidouri et al., 2010)

$h_{c,g-a}$ = 6.15Vv if Vv > 5 m/s

$h_{c,g-a}$ = 2.8+3Vv if Vv < 5 m/s

Where Vv is the wind speed (m/s)

The heat flux exchanged by convection between the nanofluid and the glass is given by Elsheikh et al (2019)

$q_{c,nf-g}$ = $h_{c,nf-g}$ (T_{nf}-T_g)

The convective exchange coefficient $h_{c,nf-g}$ is expressed by Hidouri el al (2019).

$$h_{c,nf-g} = 0.884\left[(T_{nf} - T_g) + \frac{(P_{nf} - P_g)(T_{nf} + 273)}{(268900 - P_{nf})}\right]^{1/3}$$

T_{nf} and T_g being respectively the temperatures of the water and the glass (inner face),

P_{nf} and P_g are the partial pressures of the nanofluid and the glass respectively and they are given by Elsheikh et al. (2019).

$$P_{nf} = \exp\left[25.317 - (\frac{5144}{T_{nf} + 273})\right]$$

$$P_g = \exp\left[25.317 - (\frac{5144}{T_g + 273})\right]$$

The heat flux exchanged by convection between the pool and the nanofluid is:

$q_{c,b-nf}$ = $h_{c,b-nf}$ (T_b-T_{nf})

T_b being the pool temperature.

Usually the convective exchange coefficient $h_{c,b-nf}$ appears in the Nusselt number (Hidouri et Mohanraj, 2019)

$$h_{c,b-nf} = \frac{k_{nf}}{L} Nu$$

According to Khaoula and Mohanraj(2019), the Nusselt number is a function of the Grashoff and Prandlt numbers.

That is :

$$Nu = f(Gr\,Pr)$$

The Nusselt number (Nu) is calculated from the multiplication of the Grashoff number (Gr), which represents the ratio of the buoyant force to the viscous force in a fluid, by the number Prandtl (Pr), which is

the ratio of kinematic viscosity $\nu = \dfrac{\mu_{nf}}{\rho_{nf}}$ to mass

thermal diffusivity $D = \dfrac{\lambda_{nf}}{\rho_{nf} Cp_{nf}}$

Where μ_{nf}, Cp_{nf} and λ_f are the dynamic viscosity, specific heat capacityand thermal conductivity respectively.

So the Nusselt number is written as follows:

$$Nu = C(Gr\,Pr)^n$$

Such that c and n are constant functions of the Grashoff number (Jaokob, M. et Gupta, 1954)

$$\begin{cases} Gr<10^3;\ C=1\ and\ n=0 \\ 10^4< Gr < 3.2\ 10^5;\ C=0.21\ and\ n=1/4 \\ 3.2\ 10^5< Gr <10^7;\ C=0.075\ and\ n=1/3 \end{cases}$$

The Grashoff number is given by Akrout et al. (2020):

$$Gr = \frac{\beta_{nf}g\rho_{nf}^2 L^3(T_b - T_{nf})}{\mu_{nf}^2}$$

With:

β: Coefficient of thermal expansion of water.

L: the depth of the water

The Prandtl number is given by Dhivagar et al. (2020),

$$Pr = \frac{\mu_{nf}Cp_{nf}}{\lambda_{nf}}$$

The exchange by convection of the nanofluid with the evaporator is written according to the following relationship

$q_{c,\,nf\text{-}e} = h_{c,nf\text{-}e}(T_{nf}\text{-}T_e)$

Hence the heat exchange coefficient, by convection between the nanofluid and the evaporator, is given by:

$$h_{c,nf-e} = 0.884\left[(T_{nf} - T_e) + \frac{(P_{nf} - P_e)(T_{nf} + 273)}{(268900 - P_{nf})}\right]^{1/3}$$

With always Pnf and Pe are the partial pressures of the nanofluid and the evaporator

$$P_{nf} = \exp\left[25.317 - (\frac{5144}{T_{nf} + 273})\right]$$

$$P_e = \exp\left[25.317 - (\frac{5144}{T_e + 273})\right]$$

6.8 Heat fluxes exchanged by radiation

The different components of the still change heat by radiation as follows:

Between the nanofluid and the glass, the heat exchange by radiation is expressed by the following relationship:

$q_{r,nf\text{-}g} = h_{r,nf\text{-}g}(T_{nf}\text{-}T_g)$

That is:

$h_{r,nf\text{-}g} = \sigma.\ \varepsilon_{eff}.((T_{nf}+273)^4 - (T_g+273)^4)$

Where ε_{eff} is the effective emissivity given, by R.L. Hamilton, O.K. Crosser (1962), as follows:

$$\varepsilon_{eff} = (\frac{1}{\varepsilon_{nf}} + \frac{1}{\varepsilon_g} - 1)^{-1}$$

ε_{nf} and ε_g are the emissivities of the nanofluid and the glass respectively.

σ, Stephan Boltzmann's constant, equal to $5.669 \cdot 10^{-8}$ W/m²K⁴

The pane transfers heat to the outside by radiation according to the relationship (Elsheikh et al. 2019),

$q_{r,g\text{-}sky} = h_{r,g\text{-}sky}(T_g\text{-}T_{sky})$

The heat transfer coefficient hr,g-sky between the glass and the sky is given by:

$$h_{r,g-sky} = \varepsilon_{eff}\sigma\frac{((T_g + 273)^4 - (T_{sky} + 273)^4)}{T_g - T_{sky}}$$

The sky temperature T_{sky} is given by Zurigat and Abu-Arabi(2004), it is expressed by the following relationship:

$T_{sky} = Ta\text{-}6$

6.9 Heat fluxes exchanged by evaporation

The heat flux exchanged by evaporation between the nanofluid and the glass is expressed by the following relationship, Hidouri el al (2010):

$q_{e,nf\text{-}g} = h_{e,nf\text{-}g}(T_{nf}\text{-}T_g) = 16.273.10\text{-}3\ h_{c,nf\text{-}g}(P_{nf}\text{-}P_g)$

Hence the exchange coefficient by evaporation is given by:

$$h_{e,nf-g} = \frac{16.273.10^{-3}h_{c,nf-g}(P_{nf} - P_g)}{T_{nf} - T_g}$$

The evaporator receives heat by evaporation of the nanofluid according to the relationship:

$q_{e,nf\text{-}ev} = h_{e,nf\text{-}ev}(T_{nf}\text{-}T_{ev}) = 16.273.10^{-3}h_{c,nf\text{-}ev}(P_{nf}\text{-}P_{ev})$

The exchange coefficient by evaporation is given by:

$$h_{e,nf-ev} = \frac{16.273.10^{-3}h_{c,nf-ev}(P_{nf} - P_{ev})}{T_{nf} - T_{ev}}$$

Mass transfer is accompanied by heat transfer called latent heat transfer, so we can write

$q_{e,tot} = m_e.L_v$

With:

m_e is the amount of distilled water produced and Lv is the latent heat of evaporation.

The total quantity of heat exchanged by evaporation is that exchanged from the nanofluid to the glass on the one hand and from the nanofluid to the evaporator on the other hand and is given by the following relations

$q_{e,tot} = q_{e,nf\text{-}g} + q_{e,nf\text{-}ev}$

That is :

$q_{e,tot} = h_{e,nf\text{-}g}(T_{nf}\text{-}T_g) + h_{e,nf\text{-}ev}(T_{nf}\text{-}T_{ev}) = m_e.L_v$

The hourly production of water is therefore expressed as:

$m_e = (q_{e,tot}.3600)/L_v$

6.10 Heat fluxes exchanged by conduction

According to Khaoula Hidouri (2014), the heat flux supplied by the condenser to the nanofluid is given by the following expression

$$q_c = \frac{COP.W}{S}$$

Where W is the power of the heat pump, W=100Watt, and COP is the coefficient of performance of the base fluid given by the following expression:

$$COP = \frac{T_{nf}}{T_{nf} - T_g}$$

7. Results and discussion
7.1 Effect of nanoparticles concentration on nanofluids temperature

The temperature values of the nanofluids, prepared by injecting of the nanoparticles into seawater (base fluid), were measured using thermocouples at different times of sunshine (from 8 a.m. to 5 p.m.). The values obtained are depicted in Fig.8 and Fig.9 which illustrates the hourly temperature variation of Al_2O_3 and Cu_2O as a function of time for three different concentrations (0.005%, 0.0075% and 0.01%) and compared with those found in the case of the Hybrid Solar Still without nanofluid (HSS without nanofluid).
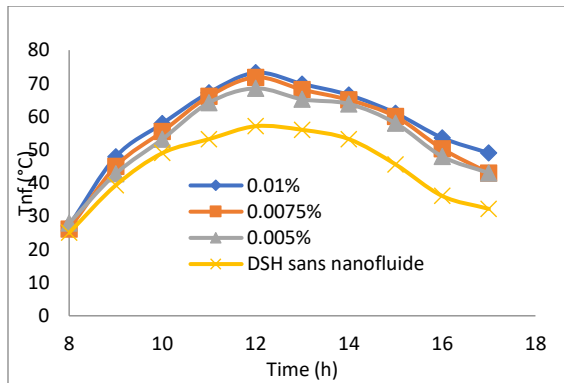

Fig. (8): Nanofluid temperature variation using Al2O3 at 0.005%, 0.0075% and 0.01% with the conventional solar still

The temperature of the base fluid with and without nanoparticles increases with the duration of sunshine from 8 a.m. to 12 p.m., after which they remain almost stable with a modest variation between 12 p.m. and 2 p.m. and decrease during the duration from 2 p.m. until 5 p.m. This phenomenon is directly related to the solar flu virus received.On the other hand, it is crucial to mention that the increase of the base fluid temperature with nanoparticles, either with Al_2O_3 or Cu_2O, is much more observable than that in the case without nanoparticles.
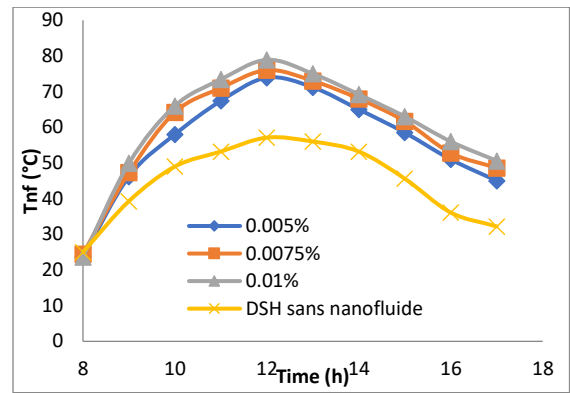

Fig. (9): Nanofluid temperature variation using Cu2O at 0.005%, 0.0075% and 0.01% with the conventional solar still

Similarly, it is observed that the temperature of the nanofluid increases more and more with the increase in the concentration of the nanoparticles in the base fluid. The maximum value is recorded with the concentration equal to 0.01%, it is around 57.1°C for the conventional still, and it reaches the values of 73.2°C and 78.9C for Al_2O_3 and Cu_2O respectively, this corresponds to a gain of 28% and 38.17%. This phenomenon can be explained by the fact that the nanoparticles can absorber solar radiation as well as the heat flow released by the heat pump in the base fluid, which causes an increase in the temperature of each nanoparticle, causing in turn an increase in thermal conductivity and fluid temperature (Sahota & Tiwari, 2016a). And as thermal conductivity is a function of the concentration of nanoparticles (Maxwell, 1891, Bruggeman, 1965 or Hamilton Crosser 1962), therefore the nanofluid temperature increases with increasing concentration.
It should be noted that the increase in the temperature of the nanofluid is much greater in the case of 0.01% as a nanoparticles concentration than that of 0.0075% and 0.005%.

7.2 Effect of the concentration of nanoparticles on the quantity of fresh water produced

The hourly evolution of the quantity of pure water produced by the hybrid solar still with only sea water and with the nanoparticles of Al_2O_3 and Cu_2O is illustrated in **Fig.10** and **Fig.11. T**hey show, clearly, that the production of pure water with the nanoparticles is much greater than that in the case without nanofluid. The addition of nanoparticles to the base fluid causes an increase in distillate production. This increase is always proportional to the increase in the concentration of nanoparticles in the base fluid; it reaches its maximum with a concentration of 0.01%. This is due to an increase in the thermal conductivity of the base fluid and the temperature, as discussed previously, and therefore heat transfer, which

generates an increase in water vapor at the surface of the nanofluid and consequently the increase in distillate production.

The difference in the amount of water produced between the two nanoparticles (Al_2O_3, Cu_2O) can be explained by the difference in its thermal conductivities and the heat capacity coefficients.
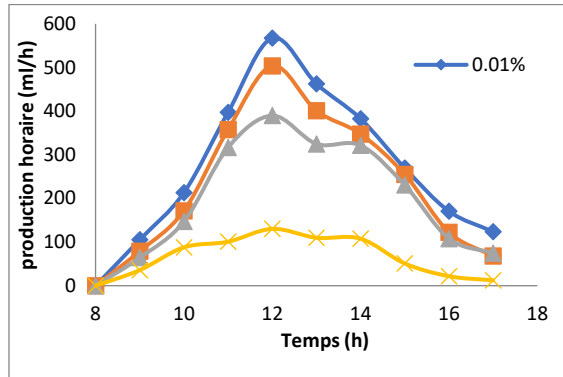

Fig.(10): Evolution of the hourly production of distilled water using Al_2O_3 at 0.005%, 0.0075% and 0.01% with the conventional solar still
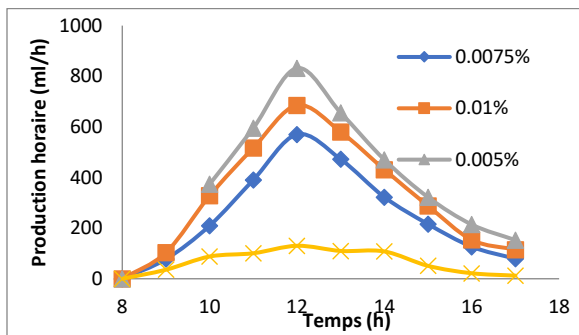

Fig. (11): Evolution of the hourly production of distilled water using Cu_2O at 0.005%, 0.0075% and 0.01% with the conventional sola

Conclusions

During this experimental study, an hybrid solar still coupled to a heat pump with and without nanofluids was studied; two types of nanoparticles, namely Al_2O_3 and Cu_2O are studied with three different concentrations φ=0.005%, 0.0075% and 0.01%.The experiments show that the temperature of the base fluid increases with the addition of nanoparticles and with the increase in their concentration. This increase in temperature is proportional to the production of fresh water and it always tends to evolve in the same way with the intensity of solar radiation. The production of the still mainly depends on the amount of heat that the salt water receives and also depends on the temperature gradient between the nanofluid and the condensing surface (inner surface of the

transparent cover and the evaporator). The amount of water recovered for the hybrid solar still with nanoparticles is greater than that with the base fluid only. In addition, the concentration of nanoparticles with which the distiller has the greatest production is φ=0.01% and the nanoparticles of dicopper oxide are evaluated as the most efficient nanoparticle always for φ=0.01%.

Symbols

m   Mass, kg
me   Mass output, kg/m2 h
P   Partial pressure, Pa
q   Heat transfer rate, W/m2
t   Time, s
T   Temperature, °C
COP   Coefficient of performance
Cp   Specific heat, J/kg K
G   Solar radiation, W/m^2
h   Heat transfer coefficient, W/m^2 K
S   Area, m^2
L   Thickness, m
k   Thermal conductivity, W/m K

Subscripts

a   Ambient
b   Basin
bf   Base fluid
c   Convection
e   Evaporative
r   Radiative
g   Glass
nf   Nanofluid
sky   Sky
i   Insulation

Greek

α   Absorptivity
τ   Transmissivity

References

[1] Akrout H., Hidouri K., Benhmidene A., Chaouachi B. Energetic, exergetic and entropic study in a simple and hybrid solar distiller. *Int. J. Ambient Energy* (2020) (17) 45274, doi: 10.1080/01430750.2020.1745274.

[2] Bruggeman (1965), Calcul de diverses constantes physiques de substances hétérogènes. Constantes diélectriques et conductivités des corps mixtes de substances isotropes,

[3] Das P.K., Islam, N., Santra, A.K., Ganguly, R. Experimental investigation of thermophysic properties of Al2O3–water nanofluid: Role of surfactants. *Journal of Molecular Liquids*. 2017. (237) 304-312. DOI: 10.1016/j.molliq.2017.04.099.

[4] Dhivagar R., Mohanraj M., Hidouri K., Belyayev Y. Energy, exergy, economic and enviro- economic

(4E) analysis of gravel coarse aggregate sensible heat storage-assisted single-slopesolar still. *Journal Thermal. Analyses and Calorimetrie*. 2020 (145) 1–22, doi: 10.1007/s10973-020-09766.

[5] Dhivagar R., Mohanraj M., Hidouri K., Midhun M., CFD modeling of a gravel coarse aggregate sensible heat storage assisted single slope solar still, *Desalination Water and Treatment.* 2021 (210) 54–69.

[6] Elango T., Kannan A., K. Kalidasa K.M. Performance studies on single basin single slope solar till with different water nanofluids, *Desalination.*2015 *(*360) 45–51.

[7] Einstein A., Investigations on the Theory of The Brownian Movement, Dover, New York, 1956.

[8] Hidouri K, Ben Slama R, Gabsi S. Hybrid solar still by heat pump compression. *Desalination 2010* (250) 444–449.

[9] Hamilton R.L. , Crosser O.K. Thermal conductivity of heterogeneous two component systems. *Industrial and Engineering Chemistry Fundamentals*1962 1(3), 187-191

[10] Kabeel A.E. , Omara Z.M, Essa F.A. Enhancement of modified, solar still integrated with external condenser using nanofluids:an experimental approach, *Energy Convers.Manage*. 2014 (78) 493–498

[11] Kabeel, A.E., Omara, Z.M., Essa, F.A. Enhancement of modified solar stillintegrated with external condenser using nanofluids: An experimental approach. *Energy Conversion and Management*. 2014a (78) 493-498. DOI: 10.1016/j.enconman.2013.11.013.

[12] Kabeel, A.E., Omara, Z.M., Essa, F.A. 2014b. Improving the performance of solar still by using nanofluids and providing vacuum. Energy Conversion and Management. 2014b (86) 268-274. DOI: 10.1016/j.enconman.2014.05.050.

[13] Khaoula K., Mohanraj M. Thermodynamic analysis of a heat pump assisted active solar still, *Desal. Water Treat*. (2019. (154) 101–110.

[14] Khaoula H. Etude thermique d'un distillateur solaire avec pompe à chaleur, National engineering school of Monastir, University of Monastir December 2014.

[15] Khaoula H., Mohanraj M. Thermodynamic analysis of a heat pump assisted active solar still, *Desal. Water Treat.* 2019. (154) 101–110.

[16] Khairul, M.A., Shah, K., Doroodchi, E., Azizian, R. & Moghtaderi, B. Effects of surfactant on stability and thermo-physical properties of metal oxide nanofluids. *International Journal of Heat and Mass Transfer*.2016 (98) 778-787. DOI:10.1016/j.ijheatmasstransfer.2016.03.079

[17] Maxwell J.C. A Treatise on electricity and magnetism, Clarendon Press, U.K., 1891.

[18] Mojarrad, M.S., Keshavarz, A., Ziabasharhagh, M. & Raznahan, M.M. Experimental investigation on heat transfer enhancement of alumina/ water and alumina/water–ethylene glycol nanofluids in thermally developing laminar flow. *Experimental Thermal and Fluid Science*. 2013 (53)111-118..

[19] Peng G., Ding H., Sharshir S.W, Li X., Liu, Ma H.D., Wu L., Zang J.. Low-cost high-efficiency solar steam generator by combining thin film evaporation and heat localization: Both experimental and theoretical study. *Appl. Therm. Eng*. 2018. (143) 1079–1084.

[20] Panitapu, B., Koneru, V., Sagi, S.L.S., Parik, A. Solar distillation using nanomaterial.*International Journal of Science, Engineering and Technology*.2014 3 (5): 583- 587.Available: https://ijset.com/ijset/publication/v3s5/IJSET_2014_5 29.pdf

[21] Jaokob, M., Gupta, P. C. Chemical engineering progress. In : Symposium series 1954.

[22] Tiwari A.K., R.P Chhabra R.P. Effect of orientation on the steady laminar free Convection heat transfer in power-law fluids from a heated triangular cylinder. *Numerical Heat Transfer.2014* (65) 780-801

[23] Sahota, L. & Tiwari, G.N. Effect of nanofluids on the performance of passive double slope solar still: A comparative study using characteristic curve. *Desalination*. 2016a 388: 9-21.DOI: 10.1016/j.desal.2016.02.039.

[24] Zurigat Y.H., Abu-Arabi M.K. Modelling and performance analysis of a regenerative solar desalination unit. *Applied Thermal Engineering*. 2004 (24) pp.1061–1072.